

Non-Kondo many-body physics in a Majorana-based Kondo type system

Ian J. van Beek and Bernd Braunecker

SUPA, School of Physics and Astronomy, University of St Andrews, North Haugh, St Andrews KY16 9SS, United Kingdom

(Received 28 June 2016; published 12 September 2016)

We carry out a theoretical analysis of a prototypical Majorana system, which demonstrates the existence of a Majorana-mediated many-body state and an associated intermediate low-energy fixed point. Starting from two Majorana bound states, hosted by a Coulomb-blockaded topological superconductor and each coupled to a separate lead, we derive an effective low-energy Hamiltonian, which displays a Kondo-like character. However, in contrast to the Kondo model which tends to a strong- or weak-coupling limit under renormalization, we show that this effective Hamiltonian scales to an intermediate fixed point, whose existence is contingent upon teleportation via the Majorana modes. We conclude by determining experimental signatures of this fixed point, as well as the exotic many-body state associated with it.

DOI: [10.1103/PhysRevB.94.115416](https://doi.org/10.1103/PhysRevB.94.115416)

Majorana zero modes have attracted significant interest in recent years [1–4] due in no small part to their potential for realizing topologically protected quantum computing architectures [5,6]. A variety of systems have been proposed, and in part experimentally implemented, to host Majorana modes, including superconductor contacted topological insulators [7], semiconductor nanowires with strong spin-orbit interaction [8–16], magnetic adatom chains on superconductors [17–32], and coupled Josephson junction arrays [33–35].

In this paper we assume the existence of such a Majorana system, for instance, in the nanowire setup depicted in Fig. 1, in which Majorana modes appear at the wire ends as a result of spin-orbit interaction in the wire, an applied magnetic field, and superconductivity induced through contact to an s -wave superconductor [8–10]. Furthermore, we consider a floating superconductor so that there is a charging energy E_C associated with the tunneling of electrons to and from the nanowire. Several studies have been performed on the low-energy behavior of such a system, predicting distinctive non-local transport and Coulomb-blockade phenomena [36–44]. The latter of these appears to have been confirmed in a recent experiment [45]. A coupling of several such Majorana wires through a common floating superconductor gives rise to the topological Kondo effect [46–54]. This is a result of the existence of Majorana modes in combination with constrained fluctuations due to a charging energy E_C . A Majorana mode may also be coupled to a quantum dot to explore the competition between Kondo and Majorana physics [55–58]. However, these works do not fully explore the potential of the Majorana modes as a novel interface between the topological superconductor and its environment.

In this work, we show that such an exploration reveals fundamentally new physics in which the Kondo and Majorana aspects combine and lead to a new type of many-body state. This marriage of traditionally distinct physics leads us to call the result the *Kondorana* model.

We consider a single Majorana wire as shown in Fig. 1 and tune it to degeneracy of two different charging states, such that tunneling into the Majorana states can make a transition between the degenerate states or lead to a high-energy ($2E_C$) excitation. By integrating out the latter, we obtain an effective Kondo-like low-energy theory, in which the two degenerate charging states take the role of the Kondo

spin S . However, the situation differs from the Kondo model in two essential ways: First, a Kondorana spin flip is induced by electron tunneling and not by an electron-spin-flip-type process. Second, the effective S^z interaction couples not to the electron spin but to a pseudospin s constructed from the electron operators for the left and right leads. In addition to the regular $S^z s^z$ coupling, the teleportation property of the Majorana states [36] leads to a further $S^z s^y$ coupling. Due to the latter, the renormalization group flow for the interaction strength has a zero eigenvalue and hence the fixed point of this Kondorana model is finite and does not lie at zero or infinity as for the Kondo model. Nevertheless, this fixed point describes a many-body state extending across the metallic leads, superconducting condensate, and Majoranas. It is important to note that the Kondorana fixed point is distinct from that found in the two-channel Kondo model [59], despite superficial similarities arising from the invocation of Majorana modes to solve the latter scenario [60,61]. Finally, we determine how the conductance of the nanowire scales with the ratio of tunneling couplings and with the temperature, and we suggest signatures of this state that should be observable with current experimental techniques.

After completion of this work we became aware of Ref. [62] in which a similar setup was investigated in a time-reversal-invariant topological superconductor with two Majorana states at each end of the wire. Remarkably, instead of Kondorana physics, a two-channel Kondo model is obtained in this system.

I. MODEL

Our analysis is based on the Majorana single-charge transistor (MSCT) [37,38], which results from the usual Majorana setup of a quantum wire with strong spin-orbit interactions in a magnetic field, but where the coupled superconductor is mesoscopic and floating, with a charging energy E_C , where $E_C \ll \Delta_{TS}$, with Δ_{TS} being the proximity-induced gap of the topological superconductor. We furthermore assume that E_C is large compared with all other energy scales, notably the tunnel couplings t_1 and t_2 to the leads, temperature T and applied voltage bias V . This system is described by the Hamiltonian $H = H_{el} + H_T + H_C$. The leads are treated as noninteracting reservoirs, $H_{el} = \sum_{j,k,\sigma} \epsilon_{jk} c_{jk\sigma}^\dagger c_{jk\sigma}$, where $c_{jk\sigma}$ are electron operators for leads $j = 1, 2$, momenta k , and spins $\sigma = \uparrow, \downarrow$,

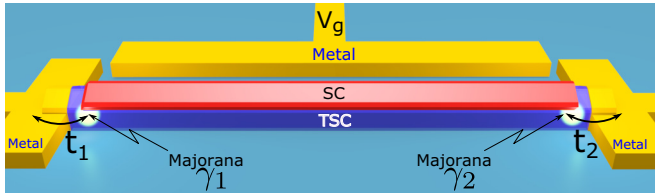


FIG. 1. A Majorana system with a floating superconductor. An s -wave superconductor (red) is grown on a nanowire with strong spin-orbit coupling (blue). For sufficiently large applied magnetic field and appropriate chemical potential the nanowire becomes a topological superconductor (TSC) with Majorana bound states γ_1 and γ_2 at each end. A gate at voltage V_g is used to tune the ground-state occupation number, which is dictated by the capacitive charging energy E_C . The nanowire couples to leads at either end with tunneling coefficients t_1 and t_2 between lead electrons and γ_1 and γ_2 .

with the dispersion ϵ_{jk} . The coupling between the leads and the superconductor is restricted to tunnelling into the Majorana states γ_1 and γ_2 , and we explicitly exclude the possibility of exciting quasiparticles [44]. The tunneling Hamiltonian can then be written as [38] $H_T = \sum_k (t_1 c_{1k\downarrow}^\dagger \eta_1 + i t_2 c_{2k\uparrow}^\dagger \eta_2) + \text{H.c.}$ We note that tunneling through the Majoranas is spin polarized [9,63], for instance, with opposite spins for both Majoranas if the magnetic field is applied perpendicular to the spin-orbit polarization direction, as written here. The spin polarization may also be non-antiparallel if the magnetic field is tilted or if there exists a mixture of Rashba and Dresselhaus spin-orbit coupling. For the purposes of this paper, it is only important that the coupling to the leads no longer has the spin degree of freedom. This allows us to effectively eliminate the spin index in the notations and we write $c_{1k} = c_{1k\downarrow}$ and $c_{2k} = c_{2k\uparrow}$. Furthermore, t_1 and t_2 are the tunneling amplitudes and $\eta_1 = \eta_2 = d \pm e^{-i\chi} d^\dagger$, with $d = (\gamma_1 + i\gamma_2)/\sqrt{2}$. The form of the η_1 and η_2 operators takes into account that tunnelling between Majorana and lead can occur over two channels: by removal of an electron from the fermionic state d obtained by the superposition of γ_1 and γ_2 (normal tunneling), or by splitting a Cooper pair and transferring one electron to the lead and the other electron to the d state (anomalous tunneling), as shown in Fig. 2. The removal of a Cooper pair is expressed by $e^{-i\chi}$, where χ is the superconducting phase operator, which obeys $[N_C, e^{-i\chi}] = -e^{-i\chi}$ where N_C is the Cooper pair number operator. We have deliberately omitted Andreev tunneling processes from our analysis for two reasons: First, their amplitude is proportional to t^2/Δ and so is much smaller than the amplitude t relevant for the considered processes. Second, an Andreev process changes the number of charges on the nanowire by ± 2 , leaving the system in an excited state that needs further relaxation, and so the Andreev processes exist only at higher orders. Finally, the charging state of the Majorana wire is given by $H_C = E_C(2N_C + n_d - n_g)^2$, where $n_d = d^\dagger d$ and n_g is a constant controlled by the gate voltage V_g . In contrast to Ref. [38], we do not consider any Josephson coupling to a further superconductor.

In this work, we tune n_g to the value $n_g = 2n - \frac{1}{2}$, with n an integer. This results in a charging ground-state degeneracy between the states ($N_C = n$, $n_d = 0$) and ($N_C = n - 1$, $n_d = 1$), with the next excited states at ($N_C = n$, $n_d = 1$) and

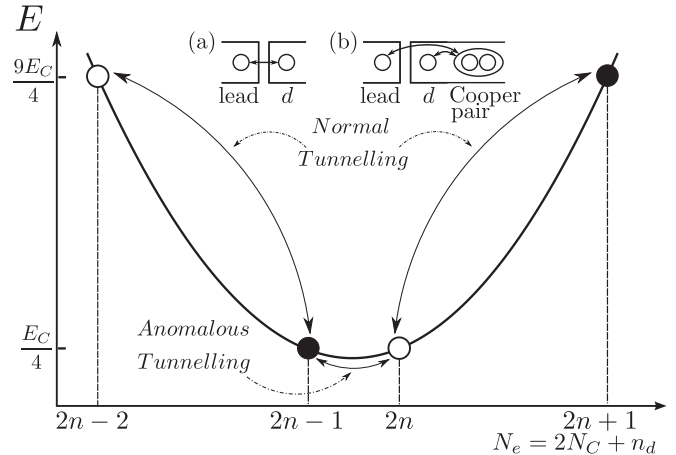


FIG. 2. Charging energy against total number of electrons, N_e , in the nanowire for $n_g = 2n - \frac{1}{2}$. Filled (empty) circles represent states with $n_d = 1$ ($n_d = 0$). Both the ground and excited states are degenerate, with transitions between them via (a) normal tunneling and (b) anomalous tunneling. Note that there is no process mediating transitions between the two excited states.

($N_C = n - 1$, $n_d = 0$) having an excitation energy $2E_C$, as shown in Fig. 2. Note that we have neglected any Majorana interaction energy, $H_{\text{int}} = \epsilon_m(n_d - 1/2)$, which would break the ground-state degeneracy. The energy ϵ_m is proportional to the Majorana wave function overlap and can be made exponentially small by a sufficiently large system size. Although this must be balanced by the requirement of maintaining a large E_C , this is not an issue since degeneracy can be restored by retuning n_g to $n_g = 2n - \frac{1}{2} - \frac{\epsilon_m}{2E_C}$. While this retuning does cause a splitting between the first-excited states of $4\epsilon_m$, the degeneracy of these states is inessential to our results and as long as $\epsilon_m \ll E_C$ this perturbation to the excited state energy is of no consequence.

Further excited states appear only at energy $4E_C$ above the first-excited states and are neglected in the present low-energy description. The resulting situation is reminiscent of the large interaction limit of the Anderson model with two-fold degenerate ground and first-excited states, yet with the restriction that there is no direct scattering process connecting the two excited states because they have different total particle numbers, $2n - 2$ and $2n + 1$. This excludes the virtual spin-flip-type processes that dominate Kondo physics, arising from the usual mapping of the Anderson model on the Kondo model, and the resulting physics for the present situation is fundamentally different. To discriminate it from the Kondo-type behavior obtained by a mutual coupling of several such Majorana wires through a common superconductor [36–44], and from the behavior of independent Majorana states, we call the effective model obtained from an analogous mapping the *Kondorana model* because it combines Kondo and Majorana properties on an equal footing but exhibits exciting new physics. We note in passing that the other charging degeneracy point, $n_g = 2n + \frac{1}{2}$, also results in a many-body state similar to the one found in this work, due to particle-like symmetry [43].

We construct the effective model through a Schrieffer–Wolff transformation, whose details are provided in Appendix A. As indicated in Fig. 2, the normal particle

tunneling between leads and Majoranas generates the high-energy excitations. Since there is no direct transition between both excited states, the virtual excitations into the high-energy sector generate an n_d -dependent scattering potential between electrons, including a teleportation-type scattering across the Majorana wire $\sim c_{1k}^\dagger c_{2k}$ [36], but do not cause any change in the Majorana parity. The resulting effective Hamiltonian is

$$\begin{aligned} H_{\text{eff}} = & H_{el} + \frac{1}{\sqrt{2}} \sum_k [(J_{\pm}^{(1)} c_{1k}^\dagger + i J_{\pm}^{(2)} c_{2k}^\dagger) S^+ + \text{H.c.}] \\ & + \sum_{k,k'} [J_z^{(11)} c_{1k}^\dagger c_{1k'} + J_z^{(22)} c_{2k}^\dagger c_{2k'} \\ & + J_z^{(12)} i(c_{1k}^\dagger c_{2k'} - c_{2k}^\dagger c_{1k})] S^z, \end{aligned} \quad (1)$$

where $S^+ = \sqrt{2}d^\dagger e^{-i\chi}$, $S^- = \sqrt{2}de^{i\chi}$, $S^z = 2n_d - 1$ are pseudospin operators, and $J_{\pm}^{(j)} = t_j$, $J_z^{(jj')} = t_j t_{j'}/2E_C$ for $j, j' = 1, 2$. A Zeeman-like term arising from the Schrieffer–Wolff transformation is omitted in Eq. (1) since it can be eliminated in the same way as ϵ_m (see above and Appendix A).

This Hamiltonian differs from the Kondo Hamiltonian in two essential ways: First, it cannot be written down as a pure spin-spin interaction because it involves the tunneling terms $J_{\pm}^{(j)}$ which create and annihilate electrons while flipping S . Second, the S^z term couples in parallel to an s^z and s^y electron pseudospin: Since the tunneling electrons have a spin polarization locked to the lead, we can define a lead-spin pseudospin with projections $s \in \{s_+, s_-\} = \{(j = 1, \downarrow), (j = 2, \uparrow)\}$ and operators $s_{k,k'}^\alpha = c_{k,s}^\dagger \sigma_{s,s'}^\alpha c_{k',s'}$ for σ^α the Pauli matrices (with σ^0 being the unit matrix). This allows us to write the S^z term as $\sum_{k,k'} [\frac{1}{2}(J_z^{(11)} + J_z^{(22)}) s_{kk'}^0 + \frac{1}{2}(J_z^{(11)} - J_z^{(22)}) s_{kk'}^z + J_z^{(12)} s_{kk'}^y] S^z$. This special form, mainly the appearance of the $s_{kk'}^y$ term, leads to a behavior of the Kondo model that is entirely different from the usual Kondo physics.

II. RENORMALIZATION

The non-Kondo behavior of the model becomes evident if we consider a renormalization group analysis. Since H_{eff} describes free electrons that are coupled to a single localized pseudospin S , the poor man's scaling technique [64] provides a transparent approach to the physics while being accurate. The renormalization incorporates the modification of the coupling constants J by virtual scattering processes to high energies. The corresponding diagrams for the $J_{\pm}^{(j)}$ coefficients are shown in Fig. 3, and details of the calculation are given in Appendix B. We obtain the scaling equations

$$\frac{d}{d\ell} \begin{pmatrix} J_{\pm}^{(1)} \\ J_{\pm}^{(2)} \end{pmatrix} = -2\rho \begin{pmatrix} J_z^{(11)} & -J_z^{(12)} \\ -J_z^{(12)} & J_z^{(22)} \end{pmatrix} \begin{pmatrix} J_{\pm}^{(1)} \\ J_{\pm}^{(2)} \end{pmatrix}, \quad (2)$$

where $\ell \sim -\ln(D/D_0)$ and $\rho \sim 1/D_0$, with D being the running cutoff energy and D_0 the initial electron bandwidth. From a similar analysis we find that $dJ_z^{(jj')}/d\ell = 0$ for all j, j' , which is a consequence of the fact that there are no $S^\pm s^\mp$ terms in H_{eff} and there are thus no $J_{\pm}^{(j)}$ terms contributing to the $J_z^{(jj')}$ renormalization.

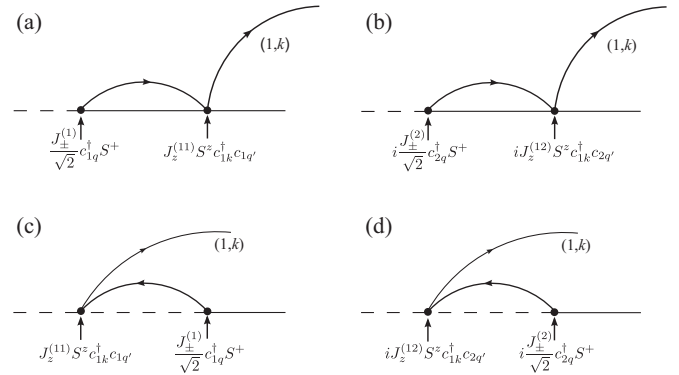


FIG. 3. Scattering channels which contribute to renormalization of $J_{\pm}^{(1)}$. Diagrams (a) and (b) show particle-mediated scattering via the left and right leads, respectively. Similarly, (c) and (d) depict hole-mediated scattering. Curved lines represent lead electrons, while the straight lines correspond to the nanowire with dashed and solid lines denoting $S_z = -1$ and $S_z = +1$, respectively.

The renormalization flow of $J_{\pm}^{(j)}$ is governed by the eigenvalues of the matrix in Eq. (2), which remain constant due to the invariance of the $J_z^{(jj')}$. Since $J_z^{(jj')} = t_j t_{j'}/2E_C$ we find that the matrix has the eigenvalues 0 and $\lambda = J_z^{(11)} + J_z^{(22)} = (t_1^2 + t_2^2)/2E_C$, such that

$$\begin{pmatrix} J_{\pm}^{(1)}(\ell) \\ J_{\pm}^{(2)}(\ell) \end{pmatrix} = \frac{t_1^2 - t_2^2}{t_1^2 + t_2^2} \begin{pmatrix} t_1 \\ -t_2 \end{pmatrix} e^{-2\rho\lambda\ell} + \frac{2t_1 t_2}{t_1^2 + t_2^2} \begin{pmatrix} t_2 \\ t_1 \end{pmatrix}. \quad (3)$$

The scaling therefore interpolates between the bare $J_{\pm}^{(j)}$ values and the fixed points $\bar{J}_{\pm}^{(1)} = 2t_1 t_2^2/(t_1^2 + t_2^2)$ and $\bar{J}_{\pm}^{(2)} = 2t_1^2 t_2/(t_1^2 + t_2^2)$, as shown in Fig. 4, and does not display the weak- or strong-coupling behavior of a regular Kondo system. Although the fixed point is finite and the Hamiltonian

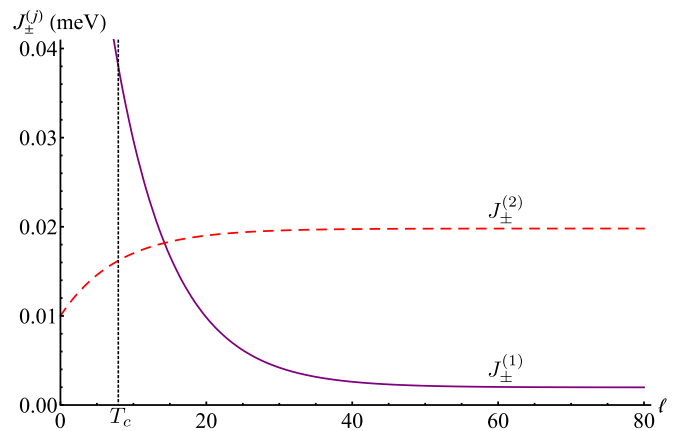


FIG. 4. Change in anomalous tunnel couplings, $J_{\pm}^{(j)}$, with scaling parameter ℓ , as given by Eq. (3) for $t_1 = 0.1$ meV, $t_2 = 0.01$ meV, and further parameters [65] based on a recent experiment [45]. The solid purple and dashed red lines show $J_{\pm}^{(1)}$ and $J_{\pm}^{(2)}$, respectively. The vertical dashed black line is the value of ℓ corresponding to the crossover temperature T_c . The couplings display a rapid, exponential change from their initial values of t_1 and t_2 as ℓ increases. This high temperature sensitivity even far above T_c is due to the large ratio $t_1/t_2 = 10$.

maintains its form, the resulting state has an involved nonlocal many-body structure. This is exemplified by the fact that the tunnel coupling asymmetry, $t_1 > t_2$, is reversed such that $t_1^* < t_2^*$ at the fixed point, showing that even for local coupling, the entire system including the leads is involved. Indeed, the state revealed above is highly nonlocal, extending over both leads regardless of nanowire length, and is comprised of lead electrons, Majorana modes, and the superconducting condensate. We believe that such a state surpasses the threshold of being merely described as dressed and requires the many-body epithet.

It must be stressed that the existence of the 0 eigenvalue is a direct consequence of the $S^z S^y$ term in the Hamiltonian, which incorporates the teleportation contribution unique to the Majorana system, and that the scaling equations (3) would be hard to obtain in any other system. In the absence of the $S^z S^y$ term, the renormalization would flow to the regular weak-coupling limit of the ferromagnetic Kondo model.

A significant consideration is whether the fixed point $\bar{J}_\pm^{(j)}$ will be reached in practice. The final value for ℓ is determined by the cutoff scale D and the renormalization stops when D becomes equal to the thermal energy $k_B T$ or any voltage bias applied to the system. The crossover scale from the bare to the renormalized values is obtained by setting $2\rho\lambda\ell \sim 1$, which resolves to

$$k_B T_c \sim D_0 e^{-1/2\rho\lambda} = D_0 e^{-E_c D_0 / (t_1^2 + t_2^2)}. \quad (4)$$

But, since the $J_\pm^{(j)}$ only renormalize for $t_1 \neq t_2$, this only makes sense for substantially different t_1 and t_2 , as otherwise the changes in $J_\pm^{(j)}$ are small. Substituting realistic system parameters [65] into Eq. (4), we notice that the flow is very slow, and practically the fixed point is never reached. Due to this it is also of little relevance if the fixed point remains finite when further corrections beyond poor man's scaling are taken into account. Such corrections have an even slower renormalization flow and are always cut off before becoming important.

III. TRANSPORT

A straightforward verification of the behavior predicted by Eq. (3) can be achieved by measuring the two-terminal conductance of the topological superconductor through the Majorana states. Neglecting terms in Eq. (1) proportional to $J_z^{(jj')}$, which are a factor t/E_C smaller than the anomalous tunneling processes, the effective tunneling Hamiltonian is given by $H_T = \sum_k [J_\pm^{(1)} c_{1k}^\dagger f + J_\pm^{(2)} c_{2k}^\dagger f + \text{H.c.}]$, where we define the composite fermion, $f = d^\dagger e^{-i\chi}$, and where the amplitudes $J_\pm^{(j)}$ are the results of the renormalization flow. If we further treat the leads in the wide-band limit, then the situation is exactly analogous to a noninteracting resonant level model, for which the (peak maximum) differential conductance at $eV < k_B T$ is [66]

$$G = K \frac{|J_\pm^{(1)}|^2 |J_\pm^{(2)}|^2}{|J_\pm^{(1)}|^2 + |J_\pm^{(2)}|^2}, \quad (5)$$

where $K = \frac{\pi^2 e^2 \rho}{hk_B T}$, with e being the electronic charge and h being Planck's constant. In principle, this conductance

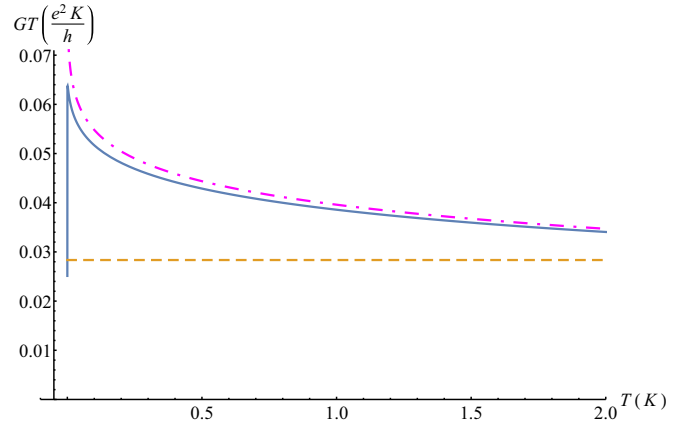


FIG. 5. Variation of conductance amplitude with temperature, adjusted to account for generic $1/T$ dependence, as given by Eqs. (3) and (5). The solid blue line depicts the result for a many-body state while the dashed orange line corresponds to the bare tunnel couplings. The dot-dashed magenta line is a high-temperature ($T \gg T_c$), high-asymmetry ($t_1 \gg t_2$) approximation, $G = K t_2^2 (e^{-2\alpha} - 4e^{-\alpha} + 4)$, where $\alpha = \ln(k_B T / D_0) / \ln(k_B T_c / D_0)$. The parameters used [65] imply $T_c = 2$ mK.

offers two signatures of the many-body state found above. First, at constant temperature T , the variation of conductance with changing t_1 , t_2 asymmetry is markedly different for $T \gg T_c$ and $T \ll T_c$. In the former case, the conductance is $G = K \frac{t_1^2 t_2^2}{t_1^2 + t_2^2}$, whereas, at low temperatures, we find that

$$G \simeq K \frac{4t_1^4 t_2^4 [t_1^2 t_2^2 + (t_1^2 - t_2^2)^2 e^{-\alpha}]}{(t_1^2 + t_2^2)^3} \text{ at } T \ll T_c, \quad (6)$$

where $\alpha = \ln(k_B T / D_0) / \ln(k_B T_c / D_0)$. However, for realistic system parameters, Eq. (6) implies that, even though T_c may be just about realizable in experiments, the temperature at which true fixed point behavior is achieved is several orders of magnitude lower.

We therefore propose a further test for the existence of a many-body state, at $T > T_c$. Fixing the system parameters, but varying T , results in a distinctive signature, as shown in Fig. 5. Here we plot the product of G and T , to remove the direct $1/T$ dependence in Eq. (5).

It is remarkable that, even at temperatures well above T_c , there is a clear difference between the scaled result and the result found from the bare tunnel couplings. That the influence of the many-body state extends to such high temperatures is a result of the strong $J_\pm^{(jj')}$ dependence in both the numerator and denominator of Eq. (6). Observation of the characteristic behavior shown in Fig. 5 appears to be within reach of current experiments and would provide compelling testament to the importance of many-body effects in this system.

IV. CONCLUSIONS

A floating topological superconductor is an obvious Majorana-based system in which to explore Kondo physics. The Majorana modes of the superconducting condensate are analogous to magnetic impurities or quantum dots in the

traditional Kondo effect, while the metallic leads fill the role of the electronic continuum.

One might initially expect this system to exhibit something close to conventional Kondo physics, possibly with a slight modification due to the Majorana modes. However, as we have shown in this work, this is not the case. By using a Schrieffer–Wolff transformation and a scaling analysis to eliminate the high-energy sectors in the wire and leads, respectively, we have demonstrated that the system flows to an intermediate fixed point, rather than the strong or weak coupling of the Kondo model. Indeed, we have shown that the presence of Majoranas is essential for this intermediate scaling to exist.

The distinct behavior arising from the interplay of Kondo and Majorana physics motivates our use of the term *Kondorana* to describe our model and the many-body state that arises from it. We have suggested possible experimental transport signatures of this state which are, in principle, within reach of current experiments.

ACKNOWLEDGMENTS

We thank C.J.F. Carroll, R. Egger, K. Grove–Rasmussen, C.A. Hooley, M. Scheurer, P. Wahl, and A.A. Zyuzin for valuable discussions and comments. I.J.vB. acknowledges studentship funding from EPSRC under Grant No. EP/I007002/1.

APPENDIX A: DERIVATION OF EFFECTIVE HAMILTONIAN

To find an effective low-energy theory of the full Hamiltonian, we carry out a Schrieffer–Wolff transformation defined by the unitary transformation $H_{\text{eff}} = e^W H e^{-W}$. This transformation is chosen such that it eliminates the tunneling processes into the high-energy sector of the model and replaces them by effective low-energy processes created by virtual high-energy excursions. With our choice of tuning the gate to the degenerate ground states ($N_C = n$, $n_d = 0$) and ($N_C = n - 1$, $n_d = 1$), the direct tunneling terms provide the excitations to the high-energy sector, given by the Hamiltonian

$$H_1 = \sum_k (t_1 c_{1k}^\dagger d + i t_2 c_{2k}^\dagger d) + \text{H.c.}, \quad (\text{A1})$$

whereas the low-energy sector is described by

$$H_0 = H_{el} + H_C + \sum_k (t_1 c_{1k}^\dagger e^{-i\chi} d^\dagger + i t_2 c_{2k}^\dagger e^{-i\chi} d^\dagger) + \text{H.c.} \quad (\text{A2})$$

Expanding the unitary transformation in W leads then to the effective Hamiltonian

$$H_{\text{eff}} = H_0 + \frac{1}{2}[W, H_1], \quad (\text{A3})$$

in which we have required $[W, H_0] = -H_1$ such that the first-order high-energy excitations vanish. This requirement has the solution

$$W = \sum_k \Xi(\epsilon_k) (t_1 c_{1k}^\dagger d - i t_2 c_{2k}^\dagger d) - \text{H.c.}, \quad (\text{A4})$$

with $\Xi(\epsilon_k) = [\epsilon_k - E_C(4N_C + 1 - 2n_g)]^{-1}$. In deriving this result we have neglected Andreev-type processes of the form $c^\dagger c^\dagger e^{-i\chi}$. Such processes are indeed generated at second

order in tunneling, but since they change the number of charges on the wire by two, they always lead to high-energy excitations and contribute to the low-energy theory only at order $O(t_j^3/E_C^2)$.

Since is always possible to choose real t_1 , t_2 (any phase can be absorbed by shifting the phases of the lead electrons through a gauge transformation), we then find that the effective Hamiltonian is given by

$$\begin{aligned} H_{\text{eff}} = & E_C(2N_C + n_d - n_g)^2 \\ & + \sum_k [\epsilon_k (c_{1k}^\dagger c_{1k} + c_{2k}^\dagger c_{2k}) \\ & + (t_1 c_{1k}^\dagger d^\dagger e^{-i\chi} + i t_2 c_{2k}^\dagger d^\dagger e^{-i\chi} + \text{H.c.})] \\ & + \sum_{k,k'} \Xi(\epsilon_k) [t_1^2 c_{1k}^\dagger c_{1k'} + t_2^2 c_{2k}^\dagger c_{2k'} \\ & - \delta_{k,k'} (t_1^2 + t_2^2) n_d + i t_1 t_2 (c_{1k}^\dagger c_{2k'} - c_{2k}^\dagger c_{1k'})]. \quad (\text{A5}) \end{aligned}$$

The term with $\delta_{k,k'}$ in the last line produces an energy shift for the n_d level, similar to an overlap integral between the two Majorana wave functions, or a Zeeman-type term for the pseudospin S^z in Eq. (1). If $\rho(\epsilon)$ is the density of states and D_0 is the electron bandwidth such that $\rho \sim 1/D_0$, we can estimate the magnitude of this term as

$$\begin{aligned} & (t_1^2 + t_2^2) \sum_{k,k'} \delta_{k,k'} \Xi(\epsilon_k) \\ & = (t_1^2 + t_2^2) \int d\epsilon \rho(\epsilon) \Xi(\epsilon) \\ & \sim -\frac{t_1^2 + t_2^2}{D_0} \ln \left[\frac{D_0 - E_C(4N_C + 1 - 2n_g)}{D_0 + E_C(4N_C + 1 - 2n_g)} \right]. \quad (\text{A6}) \end{aligned}$$

For $E_C < D_0$ this term is on the order of $O(t_j^2 E_C/D_0^2)$ and thus smaller than all other considered energies. Yet it can always be removed by a slight adjustment of n_g through the gate voltage since it plays the same role as the charging energy, and we shall set it to zero henceforth.

For the remaining effective theory, the ϵ_k term in $\Xi(\epsilon_k)$ is unimportant because it causes only small corrections for the low-energy properties, and we shall drop it in the following and use the approximation $\Xi(\epsilon_k) = \Xi = -[E_C(4N_C + 1 - n_g)]^{-1}$. We finally notice that with $n_g = 2n + 1/2$,

$$4N_C + 1 - 2n_g = \begin{cases} +2 & \text{for } (N_C = n, n_d = 0) \\ -2 & \text{for } (N_C = n - 1, n_d = 1), \end{cases} \quad (\text{A7})$$

which allows us to write $\Xi = (2n_d - 1)/2E_C$ for these two states. With these results we find that the effective Hamiltonian takes the form of Eq. (1), with the latter identities leading to the S^z pseudospin term. Deviations from Eq. (A7), such as by tuning n_g slightly away from $2n + 1/2$ due to compensation of Eq. (A6) or due to the neglected dependence of Ξ on ϵ_k cause only corrections that either remain proportional to S^z or are independent of S^z and consist only of renormalizations of the chemical potentials in the leads. Equation (1) therefore represents the generic effective Hamiltonian of the system.

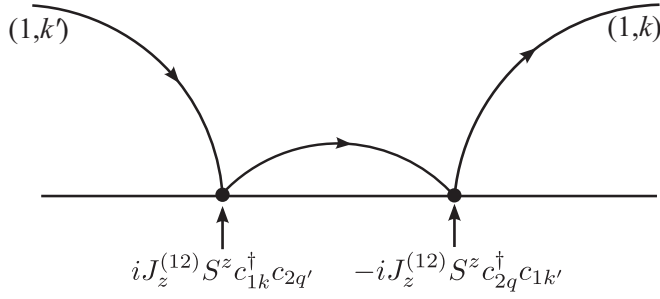


FIG. 6. The lowest-order particle mediated process contributing to the scaling of $J_z^{(11)}$. The line between the two vertices denotes a particle excited to the high-energy shell. Note that the two scattering events commute, so the pathway shown here is exactly canceled by a corresponding hole-mediated process and does not contribute to scaling.

APPENDIX B: RENORMALIZATION OF COUPLINGS

Poor man's scaling consists of a renormalization group approach in which excitations to high-energy states are successively integrated out, and the bandwidth is effectively reduced. In the following we label with q, q' these high-energy states and with k, k' the initial and final low-energy states. The renormalization proceeds by directly producing corrections to the Hamiltonian. We follow a diagrammatic variant of poor man's scaling. The first point to note is that the $J_z^{(jj')}$ couplings are invariant under scaling. The reason for this can be understood by considering Fig. 6, which shows the two vertex process contributing to the scaling of $J_z^{(11)}$.

Neither of the two vertices causes a change in Majorana parity, i.e., an S^z spin flip, and they therefore commute. The result is that the hole-mediated version of the depicted process will result in exact cancellation. Indeed, since only terms in the Hamiltonian proportional to $J_\pm^{(j)}$ change S^z , and such terms constitute terminal vertices, as shown in Fig. 3, there are no scattering diagrams, to any order, that result in scaling of $J_z^{(jj')}$.

We now turn to the scaling of $J_\pm^{(1)}$, for which the first-order scattering processes are shown in Fig. 3. The particle-mediated channels, with excitations q, q' into an energy shell of width δD at the upper band edge, lead to the following correction of

the Hamiltonian:

$$\begin{aligned} \delta H_p &= \sum_{q, q'} \left[J_z^{(11)} S^z c_{1k}^\dagger c_{1q'} (E - H_0)^{-1} J_\pm^{(1)} c_{1q}^\dagger \frac{1}{\sqrt{2}} S^+ \right. \\ &\quad \left. + i J_z^{(12)} S^z c_{1k}^\dagger c_{2q'} (E - H_0)^{-1} i J_\pm^{(2)} c_{2q}^\dagger \frac{1}{\sqrt{2}} S^+ \right] \\ &= \sum_{q, q'} \left[J_z^{(11)} J_\pm^{(1)} c_{1k}^\dagger c_{1q'} (E - D)^{-1} c_{1q}^\dagger \frac{1}{\sqrt{2}} S^+ \right. \\ &\quad \left. - J_z^{(12)} J_\pm^{(2)} c_{1k}^\dagger c_{2q'} (E - D)^{-1} c_{2q}^\dagger \frac{1}{\sqrt{2}} S^+ \right], \quad (\text{B1}) \end{aligned}$$

where E is the energy at which the system is probed and D is the running bandwidth of the leads. We have used the fact that $S^z S^+ = S^+$ and written $H_0 c^\dagger S^+ = D c^\dagger S^+$, since $|\delta D| \ll D$ and S^+ corresponds to zero-energy excitations. Summing over the high-energy interval $|\delta D|$, using the fact that $E - D \simeq -D$, and using the fact that far above the Fermi surface $c_{1q'} c_{1q}^\dagger = \delta_{qq'}$, we find that the particle-mediated contribution to the scaling is

$$\delta H_p = -\frac{\rho |\delta D|}{D} [J_z^{(11)} J_\pm^{(1)} - J_z^{(12)} J_\pm^{(2)}] c_{1k}^\dagger \frac{1}{\sqrt{2}} S^+, \quad (\text{B2})$$

where ρ is the density of states in the leads. A similar analysis for the hole-mediated terms provides an identical result, such that the total Hamiltonian associated with the two vertex events corresponding to $J_\pm^{(1)}$ is therefore

$$\delta H_{2v} = -\frac{2\rho |\delta D|}{D} [J_z^{(11)} J_\pm^{(1)} - J_z^{(12)} J_\pm^{(2)}] \frac{1}{\sqrt{2}} c_{1k}^\dagger S^+. \quad (\text{B3})$$

Comparing this with Eq. (1), we see that renormalization group flow equation for $J_\pm^{(1)}$ is

$$\frac{d}{dt} J_\pm^{(1)} = -2\rho [J_z^{(11)} J_\pm^{(1)} - J_z^{(12)} J_\pm^{(2)}]. \quad (\text{B4})$$

The derivation of the scaling for $J_\pm^{(2)}$ is essentially identical and, with Eq. (B4), gives the result shown in Eq. (2).

[1] J. Alicea, *Rep. Prog. Phys.* **75**, 076501 (2012).
 [2] M. Leijnse and K. Flensberg, *Semicond. Sci. Technol.* **27**, 124003 (2012).
 [3] C. W. J. Beenakker, *Annu. Rev. Condens. Matter Phys.* **4**, 113 (2013).
 [4] D. Aasen, M. Hell, R. V. Mishmash, A. Higginbotham, J. Danon, M. Leijnse, T. S. Jespersen, J. A. Folk, C. M. Marcus, K. Flensberg, and J. Alicea, *Phys. Rev. X* **6**, 031016 (2016).
 [5] A. Y. Kitaev, *Ann. Phys. (NY)* **303**, 2 (2003).
 [6] C. Nayak, S. H. Simon, A. Stern, M. Freedman, and S. Das Sarma, *Rev. Mod. Phys.* **80**, 1083 (2008).
 [7] L. Fu and C. L. Kane, *Phys. Rev. Lett.* **100**, 096407 (2008).
 [8] M. Sato and S. Fujimoto, *Phys. Rev. B* **79**, 094504 (2009).

[9] Y. Oreg, G. Refael, and F. von Oppen, *Phys. Rev. Lett.* **105**, 177002 (2010).
 [10] R. M. Lutchyn, J. D. Sau, and S. Das Sarma, *Phys. Rev. Lett.* **105**, 077001 (2010).
 [11] V. Mourik, K. Zuo, S. M. Frolov, S. R. Plissard, E. P. A. M. Bakkers, and L. P. Kouwenhoven, *Science* **336**, 1003 (2012).
 [12] M. T. Deng, C. L. Yu, G. Y. Huang, M. Larsson, P. Caroff, and H. Q. Xu, *Nano Lett.* **12**, 6414 (2012).
 [13] A. Das, Y. Ronen, Y. Most, Y. Oreg, M. Heiblum, and H. Shtrikman, *Nat. Phys.* **8**, 887 (2012).
 [14] L. P. Rokhinson, X. Liu, and J. K. Furdyna, *Nat. Phys.* **8**, 795 (2012).

- [15] A. D. K. Finck, D. J. Van Harlingen, P. K. Mohseni, K. Jung, and X. Li, *Phys. Rev. Lett.* **110**, 126406 (2013).
- [16] H. O. H. Churchill, V. Fatemi, K. Grove-Rasmussen, M. T. Deng, P. Caroff, H. Q. Xu, and C. M. Marcus, *Phys. Rev. B* **87**, 241401 (2013).
- [17] S. Nadj-Perge, I. K. Drozdov, B. A. Bernevig, and A. Yazdani, *Phys. Rev. B* **88**, 020407(R) (2013).
- [18] B. Braunecker and P. Simon, *Phys. Rev. Lett.* **111**, 147202 (2013).
- [19] J. Klinovaja, P. Stano, A. Yazdani, and D. Loss, *Phys. Rev. Lett.* **111**, 186805 (2013).
- [20] M. M. Vazifeh and M. Franz, *Phys. Rev. Lett.* **111**, 206802 (2013).
- [21] F. Pientka, L. I. Glazman, and F. von Oppen, *Phys. Rev. B* **88**, 155420 (2013).
- [22] K. Pöyhönen, A. Westström, J. Röntynen, and T. Ojanen, *Phys. Rev. B* **89**, 115109 (2014).
- [23] J. Röntynen and T. Ojanen, *Phys. Rev. B* **90**, 180503 (2014).
- [24] Y. Kim, M. Cheng, B. Bauer, R. M. Lutchyn, and S. Das Sarma, *Phys. Rev. B* **90**, 060401(R) (2014).
- [25] A. Heimes, P. Kotetes, and G. Schön, *Phys. Rev. B* **90**, 060507(R) (2014).
- [26] S. Nadj-Perge, I. K. Drozdov, J. Li, H. Chen, S. Jeon, J. Seo, A. H. MacDonald, B. A. Bernevig, and A. Yazdani, *Science* **346**, 602 (2014).
- [27] P. M. R. Brydon, S. Das Sarma, H.-Y. Hui, and J. D. Sau, *Phys. Rev. B* **91**, 064505 (2015).
- [28] K. Pöyhönen, A. Westström, and T. Ojanen, *Phys. Rev. B* **93**, 014517 (2016).
- [29] R. Pawlak, M. Kisiel, J. Klinovaja, T. Meier, S. Kawai, T. Glatzel, D. Loss, and E. Meyer, [arXiv:1505.06078](https://arxiv.org/abs/1505.06078).
- [30] M. Ruby, F. Pientka, Y. Peng, F. von Oppen, B. W. Heinrich, and K. J. Franke, *Phys. Rev. Lett.* **115**, 197204 (2015).
- [31] B. Braunecker and P. Simon, *Phys. Rev. B* **92**, 241410(R) (2015).
- [32] M. Schechter, K. Flensberg, M. H. Christensen, B. M. Andersen, and J. Paaske, *Phys. Rev. B* **93**, 140503 (2016).
- [33] B. van Heck, F. Hassler, A. R. Akhmerov, and C. W. J. Beenakker, *Phys. Rev. B* **84**, 180502 (2011).
- [34] B. van Heck, A. R. Akhmerov, F. Hassler, M. Burrello, and C. W. J. Beenakker, *New J. Phys.* **14**, 035019 (2012).
- [35] F. Hassler and D. Schuricht, *New J. Phys.* **14**, 125018 (2012).
- [36] L. Fu, *Phys. Rev. Lett.* **104**, 056402 (2010).
- [37] A. Zazunov, A. L. Yeyati, and R. Egger, *Phys. Rev. B* **84**, 165440 (2011).
- [38] R. Hützen, A. Zazunov, B. Braunecker, A. L. Yeyati, and R. Egger, *Phys. Rev. Lett.* **109**, 166403 (2012).
- [39] A. Zazunov and R. Egger, *Phys. Rev. B* **85**, 104514 (2012).
- [40] Z. Wang, X. Y. Hu, Q. F. Liang, and X. Hu, *Phys. Rev. B* **87**, 214513 (2013).
- [41] J. Ulrich and F. Hassler, *Phys. Rev. B* **92**, 075443 (2015).
- [42] J. D. Sau, B. Swingle, and S. Tewari, *Phys. Rev. B* **92**, 020511(R) (2015).
- [43] S. Plugge, A. Zazunov, P. Sodano, and R. Egger, *Phys. Rev. B* **91**, 214507 (2015).
- [44] S. Plugge, A. Zazunov, E. Eriksson, A. M. Tsvelik, and R. Egger, *Phys. Rev. B* **93**, 104524 (2016).
- [45] S. M. Albrecht, A. P. Higginbotham, M. Madsen, F. Kuemmeth, T. S. Jespersen, J. Nygård, P. Krogstrup, and C. M. Marcus, *Nature (London)* **531**, 206 (2016).
- [46] B. Béri and N. R. Cooper, *Phys. Rev. Lett.* **109**, 156803 (2012).
- [47] A. Altland and R. Egger, *Phys. Rev. Lett.* **110**, 196401 (2013).
- [48] B. Béri, *Phys. Rev. Lett.* **110**, 216803 (2013).
- [49] M. R. Galpin, A. K. Mitchell, J. Temaismithi, D. E. Logan, B. Béri, and N. R. Cooper, *Phys. Rev. B* **89**, 045143 (2014).
- [50] A. Zazunov, A. Altland, and R. Egger, *New J. Phys.* **16**, 015010 (2014).
- [51] A. Altland, B. Béri, R. Egger, and A. M. Tsvelik, *Phys. Rev. Lett.* **113**, 076401 (2014).
- [52] A. Altland, B. Béri, R. Egger, and A. M. Tsvelik, *J. Phys. A: Math. Theor.* **47**, 265001 (2014).
- [53] O. Kashuba and C. Timm, *Phys. Rev. Lett.* **114**, 116801 (2015).
- [54] F. Bucccheri, H. Babujian, V. E. Korepin, P. Sodano, and A. Trombettoni, *Nucl. Phys. B* **896**, 52 (2015).
- [55] M. Lee, J. S. Lim, and R. López, *Phys. Rev. B* **87**, 241402 (2013).
- [56] R. Chirla, I. V. Dinu, V. Moldoveanu and C. P. Moca, *Phys. Rev. B* **90**, 195108 (2014).
- [57] M. Cheng, M. Becker, B. Bauer, and R. M. Lutchyn, *Phys. Rev. X* **4**, 031051 (2014).
- [58] D. A. Ruiz-Tijerina, E. Vernek, L. G. G. V. Dias da Silva, and J. C. Egues, *Phys. Rev. B* **91**, 115435 (2015).
- [59] Ph. Nozières and A. Blandin, *J. Phys. (Paris)* **41**, 193 (1980).
- [60] P. Coleman, L. B. Ioffe, and A. M. Tsvelik, *Phys. Rev. B* **52**, 6611 (1995).
- [61] V. J. Emery and S. Kivelson, *Phys. Rev. B* **46**, 10812 (1992).
- [62] Z. Q. Bao and F. Zhang, [arXiv:1607.04303](https://arxiv.org/abs/1607.04303).
- [63] D. Sticlet, C. Bena, and P. Simon, *Phys. Rev. Lett.* **108**, 096802 (2012).
- [64] P. W. Anderson, *J. Phys. C: Solid State Phys.* **3**, 2436 (1970).
- [65] $D_0 = 0.4$ meV, $E_C = 0.2$ meV, $t_1 = 0.1$ meV, $t_2 = 0.01$ meV, assuming a superconducting gap exceeding E_C .
- [66] See, e.g., H. Haug and A. P. Jauho, *Quantum Kinetics in Transport and Optics of Semiconductors*, in Springer Solid State Sciences (Springer-Verlag, Berlin, Heidelberg, 1996), Vol. 123.